OPEN ACCESS Freely available online

PLOS ONE

Disruption of 3D MCF-12A Breast Cell Cultures by Estrogens – An *In Vitro* Model for ER-Mediated Changes Indicative of Hormonal Carcinogenesis

Stephanie Marchese[1], Elisabete Silva[1,2]*

1 UCL School of Pharmacy, London, United Kingdom, **2** Institute for the Environment, Brunel University, Uxbridge, United Kingdom

Abstract

Introduction: Estrogens regulate the proliferation of normal and neoplastic breast epithelium. Although the intracellular mechanisms of estrogens in the breast are largely understood, little is known about how they induce changes in the structure of the mammary epithelium, which are characteristic of breast cancer. *In vitro* three dimensional (3D) cultures of immortalised breast epithelial cells recapitulate features of the breast epithelium *in vivo*, including formation of growth arrested acini with hollow lumen and basement membrane. This model can also reproduce features of malignant transformation and breast cancer, such as increased cellular proliferation and filling of the lumen. However, a system where a connection between estrogen receptor (ER) activation and disruption of acini formation can be studied to elucidate the role of estrogens is still missing.

Methods/Principal Findings: We describe an *in vitro* 3D model for breast glandular structure development, using breast epithelial MCF-12A cells cultured in a reconstituted basement membrane matrix. These cells are estrogen receptor (ER)α, ERβ and G-protein coupled estrogen receptor 1 (GPER) competent, allowing the investigation of the effects of estrogens on mammary gland formation and disruption. Under normal conditions, MCF-12A cells formed organised acini, with deposition of basement membrane and hollow lumen. However, treatment with 17β-estradiol, and the exogenous estrogens bisphenol A and propylparaben resulted in deformed acini and filling of the acinar lumen. When these chemicals were combined with ER and GPER inhibitors (ICI 182,780 and G-15, respectively), the deformed acini recovered normal features, such as a spheroid shape, proliferative arrest and luminal clearing, suggesting a role for the ER and GPER in the estrogenic disruption of acinar formation.

Conclusion: This new model offers the opportunity to better understand the role of the ER and GPER in the morphogenesis of breast glandular structure as well as the events implicated in breast cancer initiation and progression.

Citation: Marchese S, Silva E (2012) Disruption of 3D MCF-12A Breast Cell Cultures by Estrogens – An *In Vitro* Model for ER-Mediated Changes Indicative of Hormonal Carcinogenesis. PLoS ONE 7(10): e45767. doi:10.1371/journal.pone.0045767

Editor: Irina Agoulnik, Florida International University, United States of America

Received March 21, 2012; **Accepted** August 23, 2012; **Published** October 2, 2012

Funding: Stephanie Marchese was funded by a School of Pharmacy Studentship. The funders had no role in study design, data collection and analysis, decision to publish, or preparation of the manuscript.

Competing Interests: The authors have declared that no competing interests exist.

* E-mail: elisabete.silva@brunel.ac.uk

Introduction

In recent years, three dimensional (3D) cultures of immortalised breast cells have gained immense support, as they provide a unique opportunity to model the architecture of epithelium *in vivo*, in an *in vitro* system [1,2]. Unlike monolayer cultures, immortalised mammary epithelial cells grown in 3D recapitulate numerous features of the breast epithelium *in vivo*, including the formation of growth arrested polarised acini with hollow lumen and basal deposition of basement membrane components [3,4]. These well-organised acinar structures can also reproduce important features of malignant transformation and breast cancer development *in vivo*, such as loss of apico-basal polarity, increased cellular proliferation and filling of the lumen [5] For these reasons, 3D epithelial cultures in a reconstituted basement membrane matrix (Matrigel) provide the appropriate structural and functional context for studying the events involved in the maintenance of the morphology and function of the glandular epithelium, as well as the events that trigger disruption of these structures and potentially lead to breast cancer.

Epidemiological and clinical data has provided evidence that the estrogen receptor (ER) plays an important role in the development and progression of breast cancer. Over 50% of all breast cancers express ERα and approximately 70% of those respond to therapy with anti-estrogens, such as tamoxifen, which makes the ERα an important predictor of the likelihood of a good response to hormonal therapy and overall prognosis. A role for ERα in breast cancer initiation and progression has also been suggested, as high levels of this receptor found in benign breast epithelium have been correlated with increased risk of breast cancer [6–8]. Nonetheless, a clear understanding of the involvement of the ER in breast epithelium formation, breast carcinogenesis and cancer progression is still missing, as well as the role of other estrogen-responsive receptors, such as the membrane associated G-protein coupled estrogen receptor 1 (GPER, formerly

GPR30). Although its function in the breast is still unclear, the presence and activation of GPER have been recently associated with development of tumour resistance to tamoxifen [9].

These considerations emphasise the importance of developing an *in vitro* model where the involvement of estrogen responsive receptors on breast epithelial formation and subsequent tumourigenic transformation can be studied. Establishing a system where many features of the breast epithelium can be recapitulated and a connection between ER activation and carcinogenicity can be investigated is essential to clarify the role of the ER (in particular ERα) on breast carcinogenesis, as well as the mechanisms of hormonal carcinogenesis associated with endogenous and synthetic estrogens. However, such a model has been lacking so far.

To date, investigations of the effects of estrogens in the breast in an *in vitro* 3D setting have concentrated on cultures of non-tumorigenic ERα negative/ERβ positive breast epithelial MCF-10F cells, which were derived from the floating population of the culture that also originated MCF-10A cells and share many of their characteristics [10,11]. This MCF-10F cell line has been used to investigate the effects of 17β-estradiol (E2) and its metabolites on the formation of 3D structures which characterise normal breast development. Work conducted by Russo and colleagues [12–14] has revealed that E2-treated cells lose their ability to form 3D duct-like structures in a collagen matrix, have high invasiveness and form tumours when injected into immunodeficient mice, all indicative of a cancerous phenotype. Similar observations were also reported for environmental contaminants with estrogenic activity (xenoestrogens), such as bisphenol A (BPA) and butylbenzyl phthalate (BBP) [14] and shown to derive from genomic and epigenetic changes. However, the role of ERα could not be evaluated as it is lacking in these cells.

Here, we describe an *in vitro* 3D model for breast glandular structure development, using non-transformed breast epithelial MCF-12A breast cells [15]. Unlike the alternative 3D model with MCF-12F cells mentioned above [11,14], MCF-12A cells are ERα, ERβ and GPR30 competent. This offers the opportunity to study the involvement of these receptors in breast morphogenesis, as well as the impact of ER agonists, such as estrogens and estrogen-like chemicals, on mammary gland formation, disruption and, potentially, carcinogenesis.

We observed that MCF-12A grown in matrigel under normal, control conditions formed organised, growth arrested, spheroid acini, with deposition of basement membrane components and hollow lumen. Conversely, treatment of these cells with E2 disrupted the morphology of the acini and interfered with lumen formation in a concentration-dependent manner. Interestingly, the same magnitude of effects was not observed in 3D cultures of ERα negative MCF-10A breast cells also treated with the hormone.

A similar effect to E2 was found with two xenoestrogens: BPA and the cosmetic additive n-propylparaben. Exposure of MCF-12A 3D cultures to 10 μM of these chemicals for 16 days resulted in large, misshapen, highly disorganised acini, with extensive lumen filling. The potential involvement of estrogen receptors in the described effects was evaluated by combining the test chemicals with inhibitory agents, such as the antiestrogen ICI 182,780 and the GPER antagonist G-15. Results from these co-exposures revealed that both the nuclear and the transmembrane receptors play a role in the estrogenic disturbance of acini formation, as the antagonists reversed some of effects induced by the estrogens, restoring some of the phenotypes of normal, control structures.

Results

Characterisation of receptor status of MCF-10A and MCF-12A cells and evaluation of ER target gene expression

Although the ER status of MCF-10A and MCF-12A cells has been previously published [10,16], it is widely accepted that receptor expression profiles can vary between different lots and batches of cells. As the main aim of this work was to study the effects of estrogenic chemicals in ER and GPER competent cells, it was essential to confirm the status of both receptors in the cells used here.

Our data (Figure 1A) indicated that both ER receptors (α and β) were expressed at relatively high levels in MCF-12A. In contrast, MCF-10A cells did not express measurable levels of ERα, while only very low levels of ERβ were detected. Both cell lines expressed the transmembrane GPER. Similar, confirmatory observations were made in terms of expression of the relevant genes (ERα and β and GPER) using real-time PCR (data not shown).

In order to confirm the presence of a functional ER and the response of this receptor to estrogenic treatment, the regulation of two well characterised ER-target genes was studied in both cell lines, in the presence of E2. The first gene, *TFF1* (coding for the protein pS2) has an imperfect palindromic estrogen responsive element (ERE) in its promoter region and is directly up-regulated by the activated ER. *PGR* (coding for the progesterone receptor), on the other hand, is up-regulated in the presence of estrogens due to the presence of a half-ERE site in proximity to an Sp-1 binding site [reviewed in 17].

As can be seen in figure 1B, 1 nM E2 led to a significant up-regulation of both *TFF1* and *PGR* in MCF-12A cells. The effect of the hormone was reduced in the presence of the ER inhibitor ICI 182,780, an indication of the involvement of the ER in the effects reported. Conversely, no significant regulation of either gene was observed in MCF-10A cells, which further confirms the absence of the ER in this cell line.

3D acini formation in MCF-10A cells in the presence of E2

We first investigated the effects of E2 on acini formation in MCF-10A cells, which are commonly used for 3D culture studies, but, as shown, lack ERα and present low ERβ levels.

The biological processes that contribute to the development of acinar structures in a basement membrane gel have been shown to include initial cell proliferation, deposition of the basement membrane and differentiation into two populations (outer and inner cells). This is followed by the death of the centrally located cells by apoptosis, which coincides with luminal formation [18]. Similar to previous observations [18], we found that immortalised non-malignant MCF-10A breast cells cultured for 16 days formed growth-arrested spheroid acini. These consisted of a single layer of cells (Figure 2A – cell nuclei stained blue) attached to a basement membrane (Figure 2A – basement membrane component laminin V stained red) and surrounding a hollow lumen. Some residual apoptotic cells (stained positive for activated caspase-3 - green) were still present in the centre of the lumen.

When MCF-10A cells were incubated for the same period of time with E2 (10 nM) no significant changes in the glandular structures were observed, compared to solvent controls (Figure 2). The acini were round and well organised, with a single layer of cells surrounded by a basement membrane. The lumen was completely formed, with very few residual apoptotic cells. However, in contrast to untreated cells, a small proportion of acini presented some slight filling of the lumen (Figure 2B), which

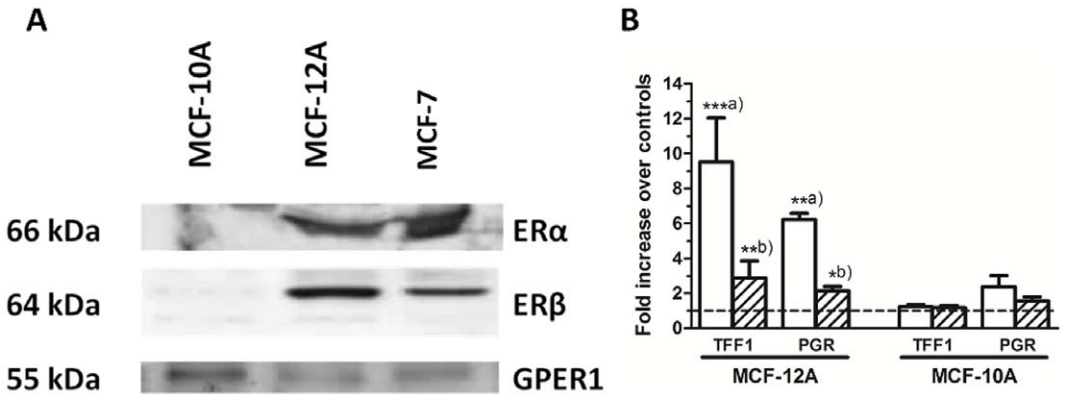

Figure 1. Receptor status and activation of ERα, ERβ and GPER in MCF-12A and MCF-10A cells. A. ERα, ERβ and GPER expression detected by immunoblotting. **B**. Regulation of ER-target genes. White bars represent treatment with 1 nM E2. Hatched white bars show the effects of E2 in combination with ICI 182,780 (1 μM). Horizontal dashed line corresponds to the negative controls (0.5% ethanol), set to 1. Data are from 3 independent experiments and error bars are mean ± SEM. **a) shows statistically significant differences ($p<0.01$) between treatments and controls. **b) ($p<0.01$) and *b) ($p<0.05$) highlight significant differences between treatments with E2 tested individually and treatments with E2 combined with ICI 182,780.
doi:10.1371/journal.pone.0045767.g001

seems to indicate a mild disruption of acini formation or maintenance.

Effects of E2 on acini formation in MCF-12A cells – dose-response studies

We repeated the experiment described above, but this time using ER competent MCF-12A cells.

In contrast to the findings with MCF-10A cells, E2 was capable of disrupting the 3D structure of MCF-12A acini in a concentration dependent fashion after treatment lasting for 16 days (Figure 3). All tested concentrations of the hormone disrupted the formation of a hollow lumen in the majority of acini. The lowest tested concentration (1 pM) affected acini morphology only weakly. At this concentration, there were generally normally shaped acini with a clear basement membrane and some lumen hollowing. At the concentrations of 10 pM and above the disrupting effects of the hormone became progressively more pronounced, with filled lumens and no apparent apoptotic cells. At 10 nM E2, the acinar structures were severely misshapen and disorganised with completely filled lumen.

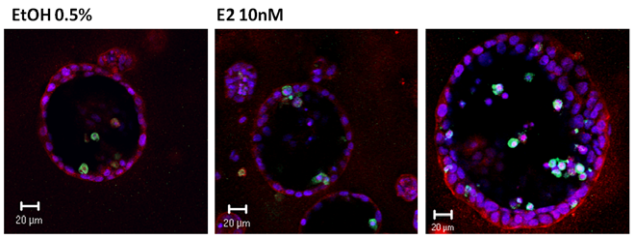

Figure 2. Confocal images of 3D cultures of epithelial breast MCF-10A cells grown in Matrigel for 16 days. Samples were either treated with solvent (ethanol 0.5%) or with 10 nM E2. Obtained structures were stained with antibody against laminin V (red) to stain the basement membrane, antibody against activated caspase-3 (green) to identify apoptotic cells and counterstained with To-PRO 3 to visualize cell nuclei (blue). Cross-sections of solvent control structures show a well delineated spheroid with a layer of viable cells in contact with the basement membrane. Two apoptotic cells are seen in the centre of the acini. **A** is representative of structures that were unaffected by estrogen treatment, as formed structures resemble those obtained in controls. **B** depicts acini that showed mild disruption after E2 treatment. Images are representative of 3 independent experiments.
doi:10.1371/journal.pone.0045767.g002

Effects of E2 and estrogen-like agents on acini formation – time course analysis

We were interested in establishing the time course for MCF-12A acini morphogenesis and investigating how the different stages in this biological process were affected by hormonal treatment. To this end, MCF-12A cells were cultured in 3D for 4, 8, 12 and 16 days in the presence and absence of E2 (1 nM) (Figure 4). Similar experiments were also carried out in the presence of the environmental estrogenic agents BPA and propylparaben (10 μM each).

In solvent-treated cultures (negative controls) the cellular organisation into spheroid structures with deposition of the basement membrane occurred almost from the onset. A full basement membrane was visible within 4 days of incubation. At this stage, acini were still small and the internal organisation was not clear, but structures were round and well formed. Within 8 days, control acini were larger in size, measuring an average of 96.4±5.2 μm in diameter (Figure 5), well organised and presented a single layer of cells in contact with the basement membrane. There was also clear evidence of lumen hollowing, as a large percentage of luminal cells stained positive for activated caspase-3, a marker for apoptosis. Further enlargement and luminal formation occurred at day 12 in control acini, when these increased in size to 102.0±4.8 μm on average. Finally, acini reached their maximum size at 16 days of incubation, with a diameter of 120.5±4.4 μm (Figure 5). At this time point, structures were also completely hollow and growth arrested, as no further enlargement was observed with longer incubation periods (data not shown).

In E2 treated samples, the progress of acini formation was clearly disrupted from very early on. At 4 days, E2 treated acini appeared organised and well formed, but were larger than those seen in the controls. After 8 days, E2 treated acini were not too dissimilar from controls, as the size of the spheroid structures, as well as the number of cells per acini, did not differ significantly from those found in untreated samples (Figure 5). However, there was an indication that luminal clearing was being affected or delayed, as the relative number of central apoptotic cells was

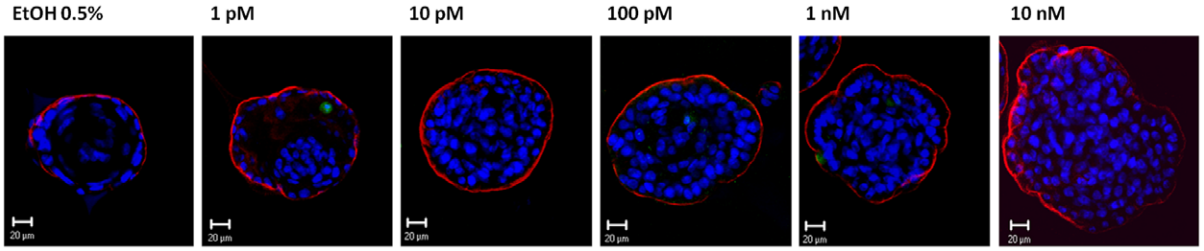

Figure 3. Dose-response analysis of 3D cultures of MCF-12A cells grown in Matrigel for 16 days in the presence of E2. Cells were either incubated with solvent (ethanol 0.5%) or with increasing concentrations of E2. Resulting samples were treated with antibodies against laminin V (red), activated caspase-3 (green) and nuclei visualized with To-PRO 3 (blue), and subsequently analysed by confocal microscopy. Images are representative of each one of the treatments and 3 independent experiments.
doi:10.1371/journal.pone.0045767.g003

reduced. As seen in figure 6, the percentage of apoptotic cells in relation to the total number of cells in the acinar structures significantly decreased from 10.7±1.8, under control conditions, to 2.46±0.66 in the presence of E2. This effect on luminal formation became even more evident after 12 days incubation. At this time, apoptosis was inhibited, as there was little or no evidence of activated caspase-3 in the central cells and the percentage of apoptotic cells had decreased to 1.6±0.4 (compared to 7.6±0.99% in controls).Finally, at 16 days the full impact of E2 treatment was seen, with the hormone inducing the formation of large, severely deformed acini with completely filled lumen. Here, acini measured an average of 142.1±3.9 μm and contained 62.3±5.9 cells, as opposed to 120.5±4.4 and 37.8±3.9, respectively, in controls. This, in combination with the distorted morphology of the structures formed, suggested excessive proliferation and indicated that cells had escaped the proliferative arrest phenotype characteristic of a control situation.

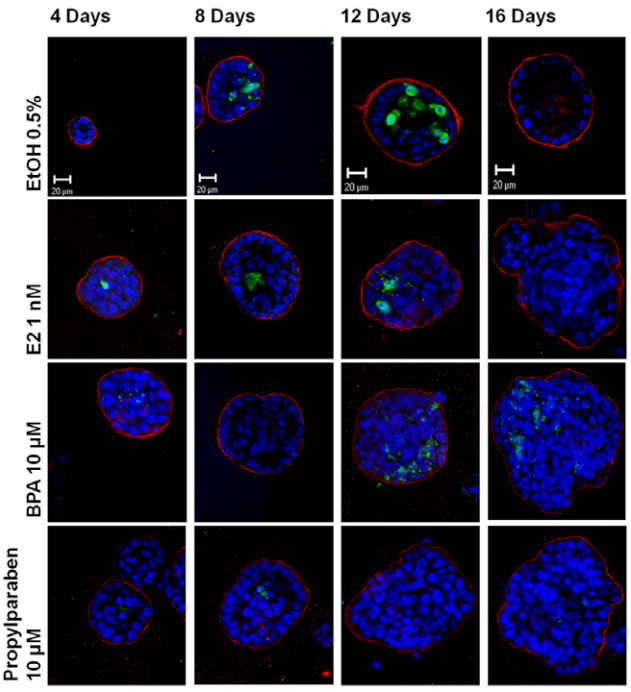

Figure 4. Time-course analysis of the formation of MCF-12A acini cultured in matrigel in the presence of the test chemicals. Cells were either treated with solvent (ethanol 0.5%) or with 1 nM E2, 10 μM BPA or 10 μM propylparaben and allowed to grow for 4, 8, 12 and 16 days. The resulting structures were immunostained with antiserum to laminin V (red) to delineate the secretion of basement membrane, activated caspase-3(green) to detect apoptotic cells and counterstained with TO-PRO 3 to visualize the cell nuclei. Confocal images are representative of 3 independent experiments.
doi:10.1371/journal.pone.0045767.g004

BPA and propylparaben, both tested at a concentration of 10 μM, had a dramatic impact on acini morphogenesis (Figure 4 and 5). Similar to the natural hormone, this effect became noticeable within 8 days of incubation, when the majority of the structures completely lacked apoptotic cells within the lumen and presented no evidence of luminal clearing. At this stage, both treatments significantly reduced the percentage of apoptotic cells found in acinar structures (Figure 6), resulting in 0.79±0.6 and 0.46±0.26% of apoptotic cells, respectively, in comparison to 10.7±1.8 in untreated controls.The differences between control and treatments became even more obvious at 12 and 16 days incubation. The resulting structures still presented deposition of basement membrane, but were significantly larger than controls (see Figure 5) and no longer had a regular spheroid shape. Cells within the acini were disorganized, there was no evident single layer of cells attached to the basement membrane and lumen were completely filled. Similar to E2, acini were not growth arrested, as they continued increasing in size throughout the treatment.

Impact of ER and GPER inhibitors on estrogen-mediated acini disruption

As all three tested compounds are known ER agonists and are able to activate GPER, we became interested in investigating whether blocking the signal from these receptors would prevent the disruptive effects of estrogens. 3D cultures of MCF-12A cells were treated with the test chemicals (E2, 1 nM; BPA, 10 μM; propylparaben 10 μM) in the presence of the ERα antagonist ICI 182,780 (1 μM), the GPER inhibitor G-15 (10 nM), or a combination of both inhibitors (ICI 182,780 1 μM + G-15 10 nM) for 16 days. The inhibitors were also tested on their own and it became apparent that they, themselves, had a small impact on acini morphology and caused some degree of acini filling (Figure 7A). Nevertheless, it was also observed that the presence of both antagonists reverted to a considerable extent the acini disruption caused by all three estrogens. As seen in figure 7, ICI 182,780 allowed E2-treated acini to regain a well organized, small, spheroid shape and some luminal clearing. A similar observation was made with G-15, the GPER inhibitor, where acini appeared slightly smaller and partially hollowed, with apoptotic luminal cells. As shown in figures 7B and 7C, although the presence of the inhibitors failed to have a dramatic impact on the size of acini (although G-15 yielded a significant effect), both inhibitors significantly decreased the number of cells found in each acini, which is reflected in the ratio cell number/acini size (Figure 7D).

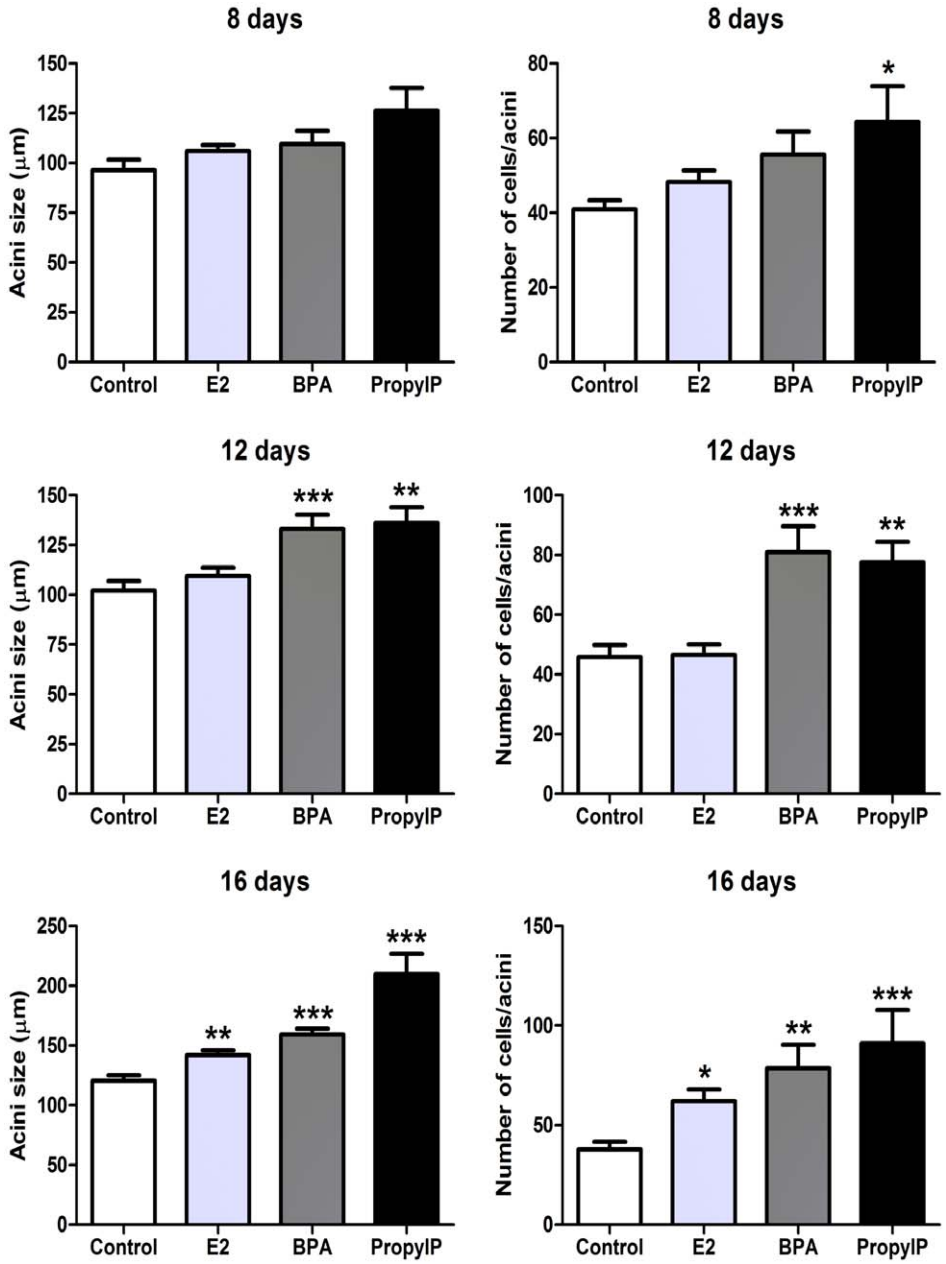

Figure 5. Quantification of acini size and cell number/acini. The size of acini (μm) and the number of cells per acini were determined by analyzing confocal images of the incubation periods of 8, 12 and 16 days. Data corresponds to mean ± SEM and results from three independent experiments, where a minimum of 10 representative acini were analysed per experiment. * ($p<0.05$), ** ($p<0.01$) and *** ($p<0.001$) indicate significant differences between treatments and controls.
doi:10.1371/journal.pone.0045767.g005

This ratio was significantly reduced for samples treated with E2 + ICI 182,780 and E2 + ICI 182,780 + G-15, in relation to those treated with E2 alone. This indicates that the reduction in cell number was not proportional to the reduction in acini size, suggesting it was related to increased hollowing and not just a consequence of smaller acini. These inhibitors also seemed to affect the deregulation of acinar formation caused by the environmental estrogens. In the case of BPA, both inhibitors caused a reduction of acini size in comparison to those resulting from BPA treatment alone (Figure 7B). Structures were also more organised and spheroidal, with some evidence of lumen hollowing, which was demonstrated by a strong reduction in cell number within acinar structures (Figure 7C) and a reduction of the ratio cell number/acini size (Figure 7D). With propylparaben, structures formed in the presence of ICI 182,780 and G-15 were smaller (Figure 7B), but still presented a completely filled lumen and no signs of apoptosis. In this case, it seemed clear that the reduction in cell number was a consequence of a reduction in acini size, and not luminal clearing, as the ratio cell number/acinar size remained similar to that determined for propylparaben alone (figure 7D).

Interestingly, the combination of ICI 182,780 and G-15 had a greater impact on the effects of E2 and BPA, yielding structures that resembled control acini in many ways. These were structurally

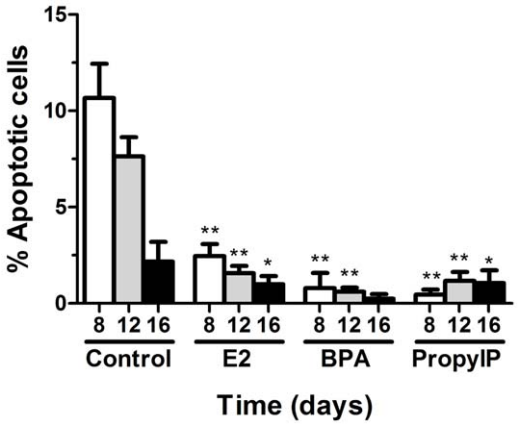

Figure 6. Quantification of the percentage of apoptotic cells per acini. The percentage of apoptotic cells was calculated for 8, 12 and 16 days incubation periods. This was determined as the number of cells positive to activated caspase-3 (stained green) over the total number of cells in each acini. Data corresponds to mean ± SEM from three independent experiments (10 acini/experiment were analysed). * ($p<0.05$) and ** ($p<0.01$) denote significant differences between treatment and controls at the corresponding incubation periods.
doi:10.1371/journal.pone.0045767.g006

organised and partially hollow, suggesting the inhibition of both ER and GPER reduced the disrupting effects of both chemicals. This was further supported by the ratio cell number/acini size, which decreased significantly for both chemicals in the presence of both inhibitors (Figure 7D), indicating a lower number of cells and, consequently, acinar hollowing. On the other hand, although the malformations caused by propylparaben were reduced by the inhibitors (especially in relation to size), apoptosis seemed largely unaffected, as acini were still completely filled and the ratio cell number/acini size remained unaltered. This highlighted the possibility that other factors might be at play here.

Discussion

For the first time, we show that the endogenous hormone E2 and the environmental estrogens BPA and propylparaben are able to disrupt the correct formation of acini in 3D cultures of ERα, ERβ and GPER competent MCF-12A normal breast cells. The extent of these abnormalities differed depending on the compound and concentration, but overall they were characterised by the formation of aberrant, highly proliferative and disorganised acini, with filled lumen. As demonstrated previously, [4,18–20] normal breast epithelial cells grown in 3D basement membrane cultures share properties with the glandular breast epithelium *in vivo* as they form hollow, organised spherical structures, with basal deposition of basement membrane and apoptotic clearance of the luminal cells. The development of large, misshapen acini with filled lumen and unregulated proliferation, as seen here in the presence of our test compounds, resembles the events that occur during the early stages of breast cancer in humans [3,21] and could, potentially, be indicative of neoplastic transformations.

Interestingly, a similar outcome was not observed in ERα negative MCF-10A cells treated with E2, where the hormone induced only mild effects, hardly distinguishable from those observed in controls. As shown here, MCF-12A differ from MCF-10A cells in that they express the ERα, raising the possibility that the marked acini disruption caused by E2 in MCF-12A cultures is somewhat dependent on the presence of ERα. This hypothesis is further supported by our observations that blocking of receptor signalling by using a combination of ICI 182,780 or G-15 with the test compounds reverted the disrupting effects of the estrogens to a large degree in MCF-12A cultures. The evidence that these inhibitors prevented, to a large extent, the damaging effects of E2, BPA and propylparaben to the 3D glandular structures, highlights a role for these receptors in the actions of estrogens (natural and man-made) in the breast glandular morphogenesis and maintenance.

Work conducted previously with MCF-10A cells has shown that the correct functioning and organisation of 3D acini depends on a fine balance between cell proliferation and cell death (apoptosis). An overstimulation or perturbation of these processes will lead to aberrations in glandular structure, such as formation of large misshapen acini with filled lumen and no apico-basal polarity [20,22–25]. To date, a number of mechanisms responsible for cell proliferation and apoptosis have been identified as playing an important role in the development and maintenance of acini. These include receptor tyrosine kinases, such as type I insulin-like growth factor receptor (IGFIR) and epidermal growth factor receptor (EGFR), signal transduction pathways, such as PI3K/Akt and Ras/Raf/Erk and cell cycle and apoptosis regulating genes, like cyclin D1 and Bcl-X_L [23–26]. Often, deregulation of acinar structures arises when one or more of these pathways are overactivated or blocked. For example, in 3D cultures of MCF-10A cells, hyperactivation of the PI3K/Akt cascade induces deregulation of acini polarity [27] as well as the disruption of cell size and proliferation, resulting in the formation of large, deformed structures. Also, when combined with an upregulation of the oncoprotein cyclin D1, the hyperactivation of PI3K/Akt or EGF signaling [22,25] promote uncontrolled cell proliferation and evasion from proliferative arrest in MCF-10A spheroids. Additionally, when these strong proliferative signals occur simultaneously with apoptosis inhibition, either by hyperactivation of anti-apoptotic genes, such as Bcl-2 or by the reduced expression of pro-apoptotic genes, such as BIM, the unregulated growth of acini is accompanied by filling of the lumen [23,26].

From the data presented here, it can be noted that the tested chemicals had an impact on both biological processes, cell proliferation and apoptosis, within the acinar structures and the blocking of the estrogen receptors (ER and GPER) seemed to preserve the original features of the spheroids, also in relation to both processes. The formation of large, deformed structures, sometimes presenting multiacinar phenotypes, indicated that the treated cells escaped proliferative arrest and were actively growing as cultures progressed. On the other hand, the reduction of cell death was evidenced by a reduced number of apoptotic cells as soon as day 8 and the completely filled lumen seen at the end of the experiment. Interestingly. The presence of the inhibitors ICI 182,780 and G-15 led to the formation of acini which were smaller in size and spheroid in shape, suggesting proliferative arrest had been restored. Moreover, especially in in the cases of E2 and BPA, luminal clearance was clearly visualised following co-incubation with ICI182,780 and ICI 182,780 + G-15. However, and in spite of the dramatic reduction in cell number in the presence of the inhibitors, these antagonists failed to completely revert the acinar filling induced by the estrogens.

In addition to the well documented direct activation of the nuclear ER and subsequent regulation of ER-target genes (genomic events), estrogens (endogenous and exogenous), such as E2 and BPA, also rapidly and transiently activate signal transduction pathways, such as the PI3K/Akt, Src/Ras/Erk and PKC cascades, via a cell membrane associated ER (non-genomic effects) [28] and GPER [29–31]. It is believed that these genomic and non-genomic pathways converge to influence cell proliferation

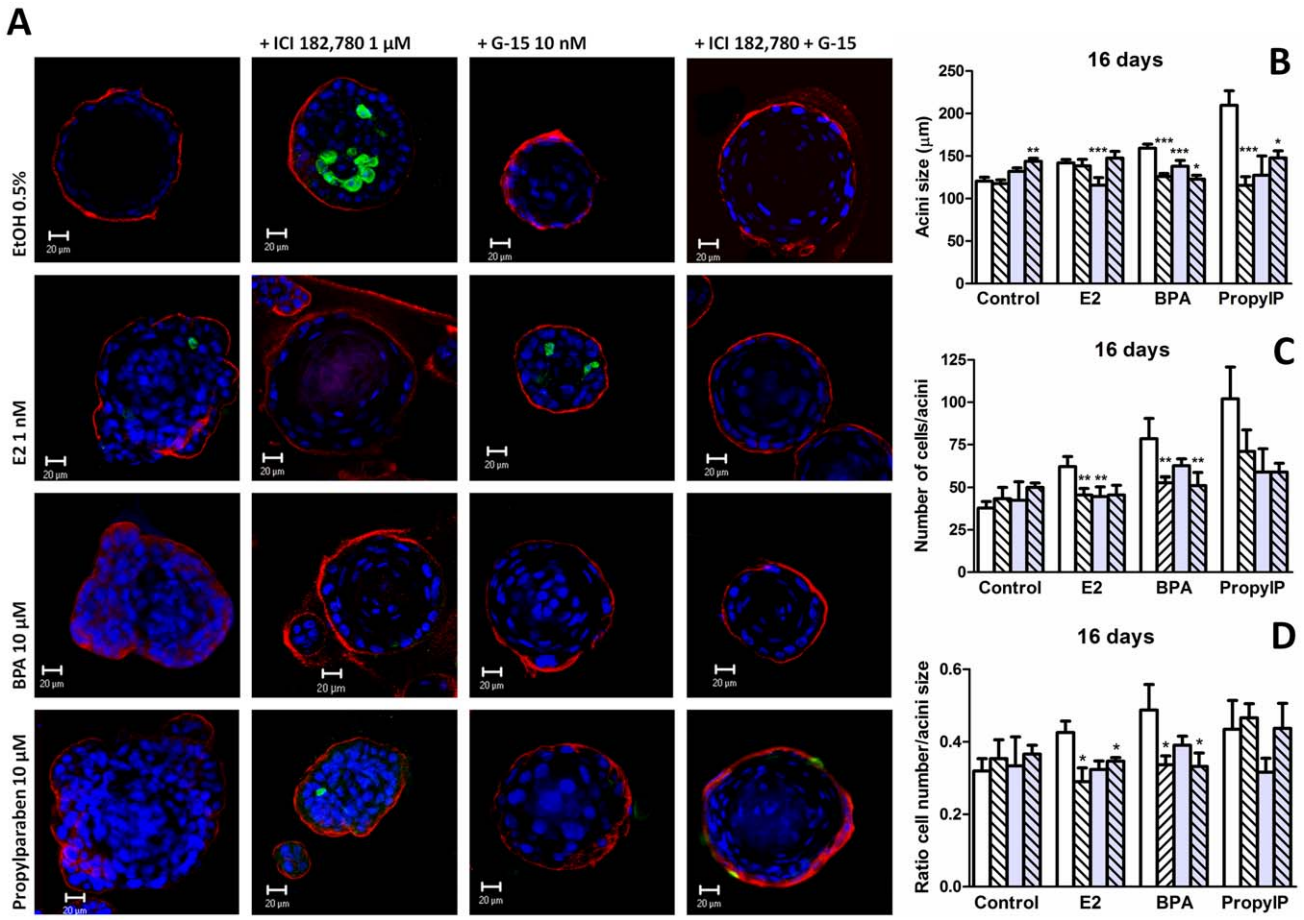

Figure 7. Impact of ER and GPER inhibitors on acini disruption by estrogens. Cells were treated with the test compounds (E2, 1 nM; BPA, 10 μM; propylparaben, 10 μM) alone or in combination with ICI 182,780 (1 μM), G-15 (10 nM) or ICI 182,780 (1 μM) + G-15 (10 nM) for 16 days. **A** Resulting acinar structures were immunostained as described before. Red shows laminin V and basement membrane deposition, green highlights apoptotic cells by staining activated caspase-3 and blue shows cell nuclei (TO-PRO 3 counterstain). Images were visualized by confocal microscopy and represent 3 experiments, run independently. **B**. Quantification of acinar size following treatment with estrogenic chemicals and inhibitors. White bars represent treatment with individual compounds. Hatched white bars show the effect of the chemicals in the presence of ICI 182,780 and grey bars of test compounds in combination with G-15. Grey hatched bars show the effect of the test chemicals when combined with ICI 182,780 + G-15. **C**. Number of cells per acini. **D**. Ratio cell number/acini size calculated for the samples shown in B and C. For all graphs, data results from three independent experiments (10 acini/experiment) and indicates mean ± SEM. * ($p<0.05$) and ** ($p<0.01$) highlight significant differences between treatments with estrogenic agents tested individually and treatments with estrogens combined with inhibitors.
doi:10.1371/journal.pone.0045767.g007

and apoptotic processes [32]. Significantly, this cross-talk between ER and growth factor signalling has also been linked to genomic instability in cancer cells [33] and the development of resistance to hormone therapy [34].

As well as the second-messenger signalling cascades mentioned above, a number of other factors known to be involved in acini maintenance and formation have also been reported to be targets of estrogenic action. For example, cyclin D1, which has been identified as an important regulator of acinar development and proliferation arrest, is also regulated by estrogens, both via the genomic and the non-genomic routes in breast cancer cells. We and others have shown that the transcription of *CCDN1* (the gene coding for cyclin D1) can be up-regulated by direct activation of the nuclear ER and in an ER-independent fashion by E2 and estrogen-like chemicals [32,35]. This culminates in an up-regulation of the cyclin D1 mRNA and protein, leading, consequently, to an increase in cell division and proliferation [36]. Similar reported targets of estrogenic activity are apoptosis regulating factors, such as Bcl-xL and Bcl-2 [37]. Estrogens increase the expression of anti-apoptotic Bcl-2 and Bcl-xL in normal and breast cancer cells, directly by interacting with the ER [38,39], and indirectly via signalling cascades, such as PI3K [40]. Environmental contaminants, such as BPA, have also been shown to activate Bcl-2 in breast cancer cells in a similar way to E2 [41]. Based on these considerations, it is plausible that the interaction of estrogens with the ER, GPER and signalling cascades in 3D cultures of normal breast cells results in similar outcomes, inducing increased cell growth and decreased cell death. The changes in this balance between cell death and survival would ultimately result in disruption of acini formation and the deformed spheroid structures reported here.

One other important point to consider is the fact that we observed that both ICI 182,780 and G-15 alone induced a small, but noticeable disruption of the normal development of acini. Toxicity of these chemicals can be ruled out, as the concentrations used were tested in monolayer cultures of MCF-12A cells and no evident cell death or toxicity was observed (data not shown). Therefore, we suspect that these effects are possibly related to

interactions of the inhibitors with targets other than their cognate receptors. For example, ICI 182,780, is a 'pure' antagonist of the ER, but also has been shown to act as an agonist potential for GPER [42]. In turn, this transmembrane receptor can interfere with signalling events controlled by EGF, which is present in the medium at low levels in order to support acini formation. As mentioned above, EGF-responsive signalling pathways, such as the Erk1/2 signalling cascade, are involved in breast structure formation and maintenance. Therefore, it is possible that by indirectly interfering with these cascades' normal function, inhibitors are causing a small degree of acinar aberrations, such as filling of the lumen, mimicking some of the responses caused by the hormones. Nevertheless, the effects caused by the inhibitors alone are minimal compared to those seen with the estrogens and do not seem to mask the reduction of acini disruption by the hormones in the co-incubation scenarios.

In light of our findings and the documented importance of signalling pathways in breast glandular maintenance, we hypothesise that the effects seen with MCF-12A cells in 3D cultures are the result of a disruption of the balance between cell proliferation and apoptosis, which, in turn, is a consequence of the effects of estrogens on the ER, GPER and extranuclear signalling cascades. Moreover, as highlighted previously by Thompson et al. [43], it is likely that ERα interplays with ERβ and membrane associated receptors, such as the GPER, to influence breast glandular maintenance, as well as mediate breast tumour development and growth [42]. This might, ultimately, disrupt acini morphogenesis and lead to the abnormal structures characteristic of early stages of breast cancer.

Work conducted by Russo and colleagues [12–14] revealed that E2 is able to induce neoplastic phenotypes in 3D cultures of MCF-10F cells. These are normal, immortalised ERα negative/ERβ positive breast cells, which are able to form 3D duct-like structures in a collagen matrix. When treated with E2, these cells lose their ductulogenic capacity, show increased invasiveness and form tumours when subsequently injected in immunodeficient mice. The treatment of the same cells with xenoestrogens, such as BPA and BBP, induced comparable effects, suggesting these compounds also have carcinogenic capabilities and could contribute to the development and progression of breast cancer. These phenotypes were shown to be associated with genetic and epigenetic changes, namely chromosomal aberrations (chromosomal loss and amplification) and DNA methylations [14]. Overall, our study provides further novel and valuable information on the effects of the endogenous hormone and xenoestrogens in 3D cultures of normal breast cells. In this context, our data supports the possibility that their interaction with the ER and possible GPER also plays a significant role, although other factors, such as genomic and chromosomal aberrations, and epigenetic changes are also likely to be associated with some of the carcinogenic characteristics of estrogenic compounds.

To this date, no major advances have been made in developing an *in vitro* assay that could link estrogenicity and ER activation with potential carcinogenicity. For example, widely used reporter gene assays for ER activation and breast cancer proliferation assays [44–46] are of great importance in screening for estrogens and defining ER affinity, but cannot be related to neoplastic events or cancer development. Although the changes in acini development and morphology reported here share many similarities with those observed in the early stages of breast cancer, it is still unclear if the abnormal acini seen in MCF12A are, in fact, representative of a neoplastic phenotype and result from neoplastic transformations induced by estrogenic compounds. Further work, fully validating this 3D *in vitro* model and characterising the nature of MCF-12A acini changes following treatment is now of utmost importance. The optimisation of a 3D system in ER competent cells, where neoplastic phenotypes can be defined and investigated, would present a valuable framework to dissect the role of the ER in breast morphogenesis and cancer development, both at cellular and tissue level. This would include investigating interaction between different types of receptors and the cross-talk between estrogens and other signalling pathways. Moreover, such a system would also provide a platform to test novel steroidal estrogen receptor modulators (SERMS) and anti estrogens, as well as study mechanisms of acquired resistance, which are still largely unknown and pose a major problem to breast cancer anti-hormonal treatment.

Materials and Methods

Chemicals

17β-estradiol (E2, 98%, Sigma-Aldrich, Dorset, UK), BPA (>99%; Sigma-Aldrich), n-propylparaben (>99%, Sigma-Aldrich) and ICI 182,780 (a kind gift from Dr. Ian White at the MRC Molecular Endocrinology Group, Leicester, UK) were solubilised in ultrapure HPLC-grade ethanol as 1 mM stocks. G-15 (Sigma-Aldrich) was prepared as 1 mM stock in DMSO. Together with subsequent dilutions, stocks were kept at −20°C, in critically clean glass containers. EGF (Sigma-Aldrich) was prepared as a 100 µg/ml stock in reconstitution solution (0.2 µm-filtered 10 mM acetic acid containing 0.1% bovine serum albumin, BSA). This solution was also stored at −20°C.

All reagents were purchased from Sigma-Aldrich unless stated otherwise.

Routine cell culture

Non-transformed breast epithelial MCF-12A and MCF-10A cells were purchased from the American Type Cell Collection (ATCC; LGC Standards, Middlesex, UK) and routinely maintained in 75 cm^2 canted-neck tissue culture flasks (Greiner, Gloucestershire, UK) in Dulbecco's Modified Eagle Medium: Nutrient Mixture F-12 (DMEM/F12, Invitrogen, Paisley, UK) supplemented with 5% horse serum (HS, Invitrogen), 20 ng/ml EGF, 0.5 µg/ml hydrocortisone, 100 ng/ml cholera toxin, 10 µg/ml insulin, 0.22 mg/ml L-glutamine and 50 µg/ml Pen/Strep (culture medium). Cells were kept in a humidified incubator, at 37°C and 5% CO_2, subcultured at approximately 70% confluence over a maximum of 10 passages and regularly tested for Mycoplasma contamination.

Preparation of cell lysates and immunoblotting

Cell lysis and immunoblotting were performed as described previously [46]. Briefly, cells were cultured in petri dishes in culture medium until 70% confluence and lysed with 200 µl 4x SDS-buffer (1 mM Tris, 20% SDS, 40% glycerol and 20% β-mercaptoethanol, pH 6.8). Protein levels were quantified using the Bradford assay. Approximately 50 µg total protein per sample were submitted to SDS-PAGE and electrophoretically transferred from the gels onto nitrocellulose membranes (Amersham, Buckinghamshire, UK) at 40 V for 1 hour. Membranes were blocked at room temperature for 1 hour in TBS-T buffer (20 mM Tris-base, 0.1 M NaCl, 0.05% (v/v) Tween-20, pH 8) with 5% skimmed milk. Incubation with primary antibody against ERα (Sigma; 1:3000 in 5% BSA/TBS-T), ERβ (Epitomics, Insight Biotechnology Ltd, Wembley, UK, 1:1000 in 5% BSA/TBS-T) and GPER (ABcam, Cambridge, UK, 1:3000 in 5% BSA/TBS-T) was carried overnight at 4°C with gentle agitation.

Blots were then washed in TBS-T three times for 5 min, incubated with secondary antibody (mouse anti-rabbit antibody, Cell Signaling Technology, New England Biolabs, Hitchin, Hertfordshire, UK, 1:2000 in 5% milk/TBS-T) and washed again following the same procedure. Detection was carried out using the ECL system according to the manufacturer's protocol (New England Biolabs) and luminescence captured by ECL hyperfilm (Amersham).

Cell treatment for RNA isolation

MCF-12A and MCF-10A cells were seeded in 25 cm^2 flasks at a density of 300,000 cells per flask and grown for 24 hours in 5 ml culture medium. Cells were then washed with 5 ml 1% Hanks' balanced salt solution without phenol-red (HBSS, Invitrogen) and changed into phenol red-free DMEM/F12 supplemented with 2% HS, 0.5 μg/ml hydrocortisone, 100 ng/ml cholera toxin, 10 μg/ml insulin, 0.22 mg/ml L-glutamine and 50 μg/ml Pen/Strep and 5 ng/ml EGF, where they were kept for further 24 hours. Medium was replaced with fresh medium containing E2 (final concentration 1 nM) or E2 (1 nM) + ICI 182,680 (1 μM), and cells treated for 24 hours. The final ethanol concentration did not exceed 0.5% (v/v). Controls were obtained by treating the cells with 5% absolute ethanol. Following the dosing period cells were harvested by the addition of 1 ml 0.25% trypsin-EDTA and incubation at 37°C for 5 minutes. The obtained cell suspension was used for RNA isolation.

RNA isolation, reverse transcription and real-time PCR

Total RNA was isolated from cell suspensions using Nucleospin RNA II (Macherey-Nagel, Abgene, Epson, UK) following the manufacturer's instructions and approximately 2.5 μg of RNA was reverse transcribed into cDNA as previously described (45). Real-time PCR was performed using iQ SYBR Green Supermix (Bio-Rad) on the CFX96 Touch Real-Time PCR Detection System (Bio-Rad). For every amplification reaction, melting curves were generated to ensure a single amplification product was obtained for each gene target. Primer pairs (Table 1) were optimised as described before (46) and purchased as high quality, purified oligos from Eurogentec Ltd (Hampshire, UK). *β-Actin* was used as internal control (reference gene) and the relative gene expression levels were calculated using comparative $2^{-\Delta\Delta C_t}$ method (47). Results were expressed as fold increase over controls, standardised such that values obtained in cells treated with vehicle only (ethanol) were set to 1. The expression ratio results were tested for statistical significance by a non-parametric Mann Whitney test.

Three-dimensional Matrigel culture

MCF-10A and MCF-12A cells were cultured in Matrigel following the protocol described by Debnath and colleagues [17], with slight modifications.

Wells in an eight-chamber slide were pre-coated with a layer of 100% growth factor reduced (GFR) Matrigel (45 μl/well) and allowed to polymerise for 15 minutes. A single cell suspension was prepared in DMEM/F12 supplemented with 2% HS, 0.5 μg/ml hydrocortisone, 100 ng/ml cholera toxin, 10 μg/ml insulin, 0.22 mg/ml L-glutamine and 50 μg/ml Pen/Strep, 5 ng/ml EGF and 2% GFR matrigel (assay medium), containing E2 (1 pM, 10 pM, 100 pM, 1 nM and 10 nM), BPA (10 μM) or propylparaben (10 μM) without exceeding the final concentration of 0.5% ethanol (solvent). For co-incubations, cells were treated with assay media containing a combination of the individual test agents (E2 1 nM, BPA 10 μM or propylparaben 10 μM) with either ICI 182,780 (1 μM), G-15 (10 nM) or a combination of both inhibitors at the same concentrations. Solvent controls were treated in assay media with ethanol at 0.5% or 0.5% ethanol + 0.2% DMSO for the treatments containing G-15. Cells were incubated for periods of up to 16 days for both cell lines, and the medium replaced every 4 days with fresh assay medium containing the test compounds. At the end of the incubation, cells were fixed and slides analysed as described below.

Immunofluorescence and confocal microscopy

Following the incubation period, the assay medium was removed from the chamber slides and cells fixed with freshly prepared 2% paraformaldehyde (in PBS, pH 7.4) for 20 mins, at room temperature. Next, cells were permeabilised with 0.5% Triton-X in PBS for 10 min at 4°C and washed three times with 100 mM glycine (in PBS) at room temperature. Acini were then blocked with immunofluorescence blocking buffer (IF buffer; 130 mM NaCl, 7.7 mM NaN3, 0.1% BSA, 0.2% Triton X-100, 0.05% Tween-20) containing 10% of goat serum for 1.5 hours at room temperature. This was followed by a secondary blocking step, where cells were incubated with IFBB containing 10% goat serum and 20 μg/ml goat anti-mouse F(ab')2 fragment for 30 mins. Primary antibodies were diluted 1:200 in the secondary block solution, incubated overnight at 4°C and rinsed three times with IF buffer. The primary antibodies used were: Mouse anti-laminin V (ABcam; 1:200 in IF buffer) and rabbit anti-cleaved caspase-3 (Cell Signaling Technology, 1:200 in IF buffer). Incubation with secondary antibody was in IF buffer containing 10% goat serum for 50 mins Dilution of 1:200), followed by three washes at room temperature. Secondary antibodies were: Alexa Fluor 488 goat anti-rabbit and Alexa Fluor 555 goat anti-mouse (Molecular Probes, Invitrogen). Cell nuclei were counterstained

Table 1. Sequence of primers for real-time PCR.

Gene	Genebank accession number	Primer	Sequence	Conc (nM)	Prod. size
β-actin	X00351	Forward	5′-TCAGCAAGCAGGAGTATG-3′	300	97
		Reverse	5′-GTCAAGAAAGGGTGTAACG-3′	300	
TFF1	NM_003225	Forward	5′-CCGTGAAAGACAGAATTG-3′	200	119
		Reverse	5′-CGATGGTATTAGGATAGAAG-3′	200	
PR	NM_000926	Forward	5′-CACAGCGTTTCTATCAACTTAC-3′	200	145
		Reverse	5′-GCAGCAATAACTTCAGACATC-3′	200	

doi:10.1371/journal.pone.0045767.t001

with 5 μM TOPRO-3 (Molecular Probes) in PBS for 15 mins, mounted with freshly prepared Prolong Antifade Reagent (Molecular probes) and allowed to dry overnight at room temp. Confocal microscopy analysis was carried our using the Carl Zeiss MicroImaging, Inc. LSM510 confocal microscopy system with LSM version 4.20. The images presented are representative of three independent experiments.

All experiments were conducted blindly throughout treatment and analysis.

Acini quantification and statistical analysis

Acini formation and disruption were quantified by analyzing confocal images of acini and measuring the size, as well as the total number of cells in a representative number of acini for each treatment. A minimum of 10 randomly selected acini were analysed for each independent experiment.

For experiments with ICI 182,780 and G-15, the ratio cell number/acini size was also calculated. This allowed for the differentiation between reduction in cell number due to acini hollowing (increased apoptosis) or due to a decrease in acini size (proliferative arrest). If the presence of an inhibitor leads to reduction in cell number due to lumen hollowing, then the ratio cell number/acini size should decrease, whereas if the number of cells decreases solely due to smaller acini, than this ratio should not suffer a major change.

Finally, the percentage of apoptotic cells was calculated as the number of cells positive to activated caspase-3 (stained green) over the total number of cells in each acini. Like before, at least 10 randomly selected acini were analysed for each independent experiment.

Data analysis was performed using the Prism Software (GraphPad Software, version 5.04, La Jolla, CA, USA). ANOVA followed by Dunnett's post-hoc test was applied to compare treatments against negative controls, while ANOVA and Bonferroni's post-hoc test was used to compare paired samples (treatments and inhibitors).

Acknowledgments

The authors would like to thank Dr David Gathercole for his support with the confocal imaging.

Author Contributions

Conceived and designed the experiments: SM ES. Performed the experiments: SM. Analyzed the data: SM ES. Contributed reagents/materials/analysis tools: SM ES. Wrote the paper: SM ES.

References

1. O'Brien LE, Zegers MMP, Mostov KE (2002) Building epithelial architecture: insights from three-dimensional culture models. Nat Rev Mol Cell Biol 3:531–537.
2. Weigelt B, Bissell MJ (2008) Unraveling the microenvironmental influences on the normal mammary gland and breast cancer. Semin Cancer Biol 18:311–321.
3. Debnath J, Brugge JS (2005) Modelling glandular epithelial cancers in three-dimensional cultures. Nat Rev Cancer 5:675–688.
4. Underwood JM, Imbalzano KM, Weaver VM, Fischer AH, Imbalzano AN, et al. (2006) The ultrastructure of MCF-10A acini. J Cell Physiol 208:141–148.
5. Harris J, Lippman M, Morrow M, Osborne C (1999) Diseases of the breast. Philadelphia: Lippicott Williams and Wilkins.
6. Khan SA, Rogers MA, Khurana KK, Meguid MM, Numann PJ (1998) Estrogen receptor expression in benign breast epithelium and breast cancer risk. J Natl Cancer Inst 90:37–42.
7. Ali S, Coombes RC (2000) Estrogen receptor alpha in human breast cancer: occurrence and significance. J Mammary Gland Biol Neoplasia 5:271–281.
8. Robbins AS, Clarke CA (2007) Regional changes in hormone therapy use and breast cancer incidence in California from 2001 to 2004. J Clin Oncol 25:3437–3439.
9. Ignatov T, Eggemann H, Semczuk A, Smith B, Bischoff J, et al.(2010) Role of GPR30 in endometrial pathology after tamoxifen for breast cancer. Am J Obstet Gynecol 203:595.e9–595.16.
10. Soule HD, Maloney TM, Wolman SR, Peterson WD, Jr, Brenz R, et al. (1990) Isolation and characterization of a spontaneously immortalized human breast epithelial cell line, MCF-10. Cancer Res 50:6075–6086.
11. Russo J, Fernandez SV, Russo PA, Fernbaugh R, Sheriff FS, et al. (2006) 17-Beta-estradiol induces transformation and tumorigenesis in human breast epithelial cells. FASEB J 20:1622–1634.
12. Russo J, Tahin Q, Lareef MH, Hu YF, Russo IH (2002) Neoplastic transformation of human breast epithelial cells by estrogens and chemical carcinogens. Environ Mol Mutagen 39:254–263.
13. Russo J, Hasan Lareef M, Balogh G, Guo S, Russo IH (2003) Estrogen and its metabolites are carcinogenic agents in human breast epithelial cells. J Steroid Biochem Mol Biol 87:1–25.
14. Fernandez SV, Russo J (2010) Estrogen and xenoestrogens in breast cancer. Toxicol Pathol 38:110–122.
15. Paine TM, Soule HD, Pauley RJ, Dawson PJ (1992) Characterization of epithelial phenotypes in mortal and immortal human breast cells. Int J Cancer 50:463–473.
16. Liu YE, Pu W, Jiang Y, Shi D, Dackour R, et al. (2007) Chaperoning of estrogen receptor and induction of mammary gland proliferation by neuronal protein synuclein gamma. Oncogene 26:2115–2125.
17. O'Lone R, Frith MC, Karlsson EK, Hansen U (2004) Genomic targets of nuclear estrogen receptors. Mol Endocrinol 18: 1859–1875.
18. Debnath J, Muthuswamy SK, Brugge JS (2003) Morphogenesis and oncogenesis of MCF-10A mammary epithelial acini grown in three-dimensional basement membrane cultures. Methods 30:256–268.
19. Mailleux AA, Overholtzer M, Brugge JS (2008) Lumen formation during mammary epithelial morphogenesis: insights from in vitro and in vivo models. Cell Cycle 7:57–62.
20. Haenssen KK, Caldwell SA, Shahriari KS, Jackson SR, Whelan KA, et al. (2010) ErbB2 requires integrin alpha 5 for anoikis resistance via Src regulation of receptor activity in human mammary epithelial cells. J Cell Sci 123:1373–1382.
21. Hebner C, Weaver VM, Debnath J (2008) Modeling morphogenesis and oncogenesis in three-dimensional breast epithelial cultures. Annu Rev Pathol 3:313–339.
22. Debnath J, Walker SJ, Brugge JS (2003) Akt activation disrupts mammary acinar architecture and enhances proliferation in an mTOR-dependent manner. J Cell Biol 163:315–326.
23. Reginato MJ, Mills KR, Becker EB, Lynch DK, Bonni A, et al. (2005) Bim regulation of lumen formation in cultured mammary epithelial acini is targeted by oncogenes. Mol Cell Biol 25:4591–4601.
24. Yanochko GM, Eckhart W (2006) Type I insulin-like growth factor receptor over-expression induces proliferation and anti-apoptotic signaling in a three-dimensional culture model of breast epithelial cells. Breast Cancer Res 8:R18.
25. Dimri M, Naramura M, Duan L, Chen J, Ortega-Cava C, et al. (2007) Modeling breast cancer-associated c-Src and EGFR overexpression in human MECs: c-Src and EGFR cooperatively promote aberrant three-dimensional acinar structure and invasive behavior. Cancer Res 67:4164–4172.
26. Debnath J, Mills KR, Collins NL, Reginato MJ, Muthuswamy SK, et al. (2002) The role of apoptosis in creating and maintaining luminal space within normal and oncogene-expressing mammary acini Cell 111: 29–40.
27. Liu H, Radisky DC, Wang F, Bissell MJ (2004) Polarity and proliferation are controlled by distinct signaling pathways downstream of PI3-kinase in breast epithelial tumor cells. J Cell Biol 164:603–612.
28. Cheskis BJ (2004) Regulation of cell signalling cascades by steroid hormones. J Cell Biochem 93:20–27.
29. Thomas P, Dong J (2006) Binding and activation of the seven-transmembrane estrogen receptor GPR30 by environmental estrogens: a potential novel mechanism of endocrine disruption. J Steroid Biochem Mol Biol 102:175–179.
30. Prossnitz ER, Arterburn JB, Smith HO, Oprea TI, Sklar LA, et al. (2008) Estrogen signaling through the transmembrane G protein-coupled receptor GPR30. Annu Rev Physiol 70:165–190.
31. Vandenberg LN, Maffini MV, Sonnenschein C, Rubin BS, Soto AM (2009) Bisphenol-A and the great divide: a review of controversies in the field of endocrine disruption. Endocr Rev 30:75–95.
32. Silva E, Kabil A, Kortenkamp A (2010) Cross-talk between non-genomic and genomic signalling pathways–distinct effect profiles of environmental estrogens. Toxicol Appl Pharmacol 245:160–170.
33. Kabil A, Silva E, Kortenkamp A (2008) Estrogens and genomic instability in human breast cancer cells–involvement of Src/Raf/Erk signaling in micronucleus formation by estrogenic chemicals. Carcinogenesis 29:1862–1868.
34. Bedard PL, Freedman OC, Howell A, Clemons M (2008) Overcoming endocrine resistance in breast cancer: are signal transduction inhibitors the answer? Breast Cancer Res Treat 108:307–317.
35. Castro-Rivera E, Samudio I, Safe S (2001) Estrogen regulation of cyclin D1 gene expression in ZR-75 breast cancer cells involves multiple enhancer elements. J Biol Chem 276:30853–30861.
36. Altucci L, Addeo R, Cicatiello L, Dauvois S, Parker MG, et al. (1996) 17beta-Estradiol induces cyclin D1 gene transcription, p36D1-p34cdk4 complex

activation and p105Rb phosphorylation during mitogenic stimulation of G(1)-arrested human breast cancer cells. Oncogene 12:2315–2324.
37. Gompel A, Chaouat M, Hugol D, Forgez P (2004) Steroidal hormones and proliferation, differentiation and apoptosis in breast cells. Maturitas 49:16–24.
38. Gompel A, Somai S, Chaouat M, Kazem A, Kloosterboer HJ, et al. (2000) Hormonal regulation of apoptosis in breast cells and tissues. Steroids 65:593–598.
39. Perillo B, Sasso A, Abbondanza C, Palumbo G (2000) 17beta-estradiol inhibits apoptosis in MCF-7 cells, inducing bcl-2 expression via two estrogen-responsive elements present in the coding sequence. Mol Cell Biol 20:2890–2901.
40. Bratton MR, Duong BN, Elliott S, Weldon CB, Beckman BS, et al. (2010) Regulation of ERalpha-mediated transcription of Bcl-2 by PI3K-AKT crosstalk: implications for breast cancer cell survival. Int J Oncol 37:541–550.
41. LaPensee EW, LaPensee CR, Fox S, Schwemberger S, Afton S, Ben-Jonathan N (2010) Bisphenol A and estradiol are equipotent in antagonizing cisplatin-induced cytotoxicity in breast cancer cells. Cancer Lett 290:167–173.
42. Filardo EJ, Quinn JA, Bland KI, Frackelton AR Jr (2000) Estrogen-induced activation of Erk-1 and Erk-2 requires the G protein-coupled receptor homolog, GPR30, and occurs via trans-activation of the epidermal growth factor receptor through release of HB-EGF. Mol Endocrinol 14:1649–1660.
43. Thompson A, Brennan K, Cox A, Gee J, Harcourt D, et al. (2008) Evaluation of the current knowledge limitations in breast cancer research: a gap analysis. Breast Cancer Res 10:R26.
44. Soto AM, Sonnenschein C, Chung KL, Fernandez MF, Olea N, et al. (1995) The E-SCREEN assay as a tool to identify estrogens: an update on estrogenic environmental pollutants. Environ Health Perspect 103 Suppl 7:113–122.
45. Wilson VS, Bobseine K, Gray LE Jr (2004) Development and characterization of a cell line that stably expresses an estrogen-responsive luciferase reporter for the detection of estrogen receptor agonist and antagonists. Toxicol Sci 81:69–77.
46. Silva E, Scholze M, Kortenkamp A (2007) Activity of xenoestrogens at nanomolar concentrations in the E-Screen assay. Environ Health Perspect 115 Suppl 1:91–97.
47. Livak K, Schmittgen T (2001) Analysis of Relative Gene Expression Data Using Real-Time Quantitative PCR and the $2^{-\Delta\Delta CT}$ Method. Methods 25: 402–408.